


## Article

# Analysis and Prediction of Wind Speed Effects in East Asia and the Western Pacific Based on Multi-Source Data

Chaoli Tang <sup>1,2</sup> , Xinhua Tao <sup>1,\*</sup>, Yuanyuan Wei <sup>3</sup>, Ziyue Tong <sup>1</sup>, Fangzheng Zhu <sup>1</sup> and Han Lin <sup>1</sup>

<sup>1</sup> School of Electrical & Information Engineering, Anhui University of Science and Technology, Huainan 232001, China

<sup>2</sup> State Key Laboratory of Space Weather, Chinese Academy of Sciences, Beijing 100190, China

<sup>3</sup> School of Internet, Anhui University, Hefei 230039, China

\* Correspondence: 2020200785@aust.edu.cn

**Abstract:** With the increasing problem of global warming caused by the massive use of fossil fuels, biomass energy as a renewable energy source has attracted widespread attention throughout the globe. In this paper, we analyzed the spatial and temporal variation in wind energy in the East Asia and Western Pacific areas using IGRA site data, ERA5, and NCEP/NCAR reanalysis data from 2000 to 2021, and multi-variate empirical orthogonal function (MV-EOF) decomposition with the Pettitt mutation test, and the seasonal autoregression integrated moving average (SARIMA) model was used to predict the trend of wind speed. The spatial and temporal variations in wind energy in East Asia and Western Pacific areas were analyzed, and it was found that the richer wind-energy resources were mainly concentrated in the “Three Norths” (North China, Northwest China, and Northeast China) and Mongolia, followed by the Western Pacific areas. In addition, the T'ai-hang Mountains and the Qinghai-Tibet Plateau in China block the wind resources in the eastern and southern regions of East Asia, resulting in a shortage of wind resources in this region. In addition, the summer wind speed is significantly lower than in the other three seasons. The first-mode contributions of the MV-EOF wind field and geopotential heights, respectively, are 29.47% and 37.75%. The results show that: (1) There are significant seasonal differences in wind-energy resources in the study area, with the lowest wind speed in summer and the highest wind speed in winter. (2) The wind energy in the study area has significant regional characteristics. For example, China's Qinghai-Tibet Plateau, Inner Mongolia, Xinjiang region, and Mongolia are rich in wind-energy resources. (3) Wind-energy resources in the study area have gradually increased since 2010, mainly due to changes in large-scale oceanic and atmospheric circulation patterns caused by global warming.

**Keywords:** wind energy; temporal and spatial variation; Pettitt test; ERA5 reanalysis; MV-EOF decomposition



**Citation:** Tang, C.; Tao, X.; Wei, Y.; Tong, Z.; Zhu, F.; Lin, H. Analysis and Prediction of Wind Speed Effects in East Asia and the Western Pacific Based on Multi-Source Data. *Sustainability* **2022**, *14*, 12089. <https://doi.org/10.3390/su141912089>

Academic Editors: Adnan Sözen, Ataollah Khanlari and Hafiz Muhammad Ali

Received: 27 July 2022

Accepted: 20 September 2022

Published: 24 September 2022

**Publisher's Note:** MDPI stays neutral with regard to jurisdictional claims in published maps and institutional affiliations.



**Copyright:** © 2022 by the authors. Licensee MDPI, Basel, Switzerland. This article is an open access article distributed under the terms and conditions of the Creative Commons Attribution (CC BY) license (<https://creativecommons.org/licenses/by/4.0/>).

## 1. Introduction

Global warming caused by greenhouse gases has long become a major environmental problem that mankind has to face. For example, global warming has caused glacier loss in the Andes from 30% to more than 50% of their area since the 1980s; the combination of continued anthropogenic disturbance, particularly deforestation, with global warming may result in the dieback of forest in the region, etc. Some academics believe that global warming is a serious threat that necessitates the global adoption of renewable-energy technologies [1]. Some researchers claim that moderately replacing fossil fuels with biofuels contributes to a reduction in CO<sub>2</sub> emissions, thereby alleviating the greenhouse effect and climate change [2]. Global warming not only destroys ecological balance but also threatens the human environment. Many scholars at home and abroad have focused their attention on clean energy (including wind, water, and solar energy), and the vigorous development of wind power, photovoltaic power generation, and other renewable energy sources have

become a broad focus in the international community to address climate change and achieve China's "double carbon" goal, as well as the use of such renewable-energy sources to solve environmental problems and energy shortages. Clean and renewable-energy sources are already becoming increasingly important for economic and environmental reasons. Wind is an essential renewable energy source [3]. The top-ten countries with the highest global carbon emissions are China, the United States, India, Russia, Japan, Germany, Iran, Canada, South Korea, and South Africa, half of which are in Asia, and three of which belong to the East Asia region. As China is currently the world's largest emitter of carbon dioxide [4], President Xi Jinping announced at the Climate Ambition Summit that China will increase its nationally determined contribution, adopt more powerful policies and measures, strive to achieve peak carbon dioxide emissions by 2030, and strive to achieve carbon neutrality by 2060, which also reflects China's firm determination to make great efforts to expand the use of clean energy [5]. The early realization of the "double carbon" goal requires the early adjustment of the energy structure, and wind energy has multiple advantages, such as renewability, wide distribution, and huge reserves. Furthermore, wind energy is one of the world's fastest-growing energy sources. This is evident from the increased number of wind-power applications in recent years. However, the unpredictability of wind speed creates several challenges in the development of efficient applications, which necessitate a thorough analysis of wind-speed data and accurate wind-energy potential at specific sites [6]. As a result, the vigorous development and assessment of wind-energy resources in China and East Asia are of great importance to achieve the "double carbon" goal.

The assessment of wind-energy resources in the study area is a prerequisite for the development and utilization of the resources in the area. Due to the different temperature changes and the different content of water vapor in the air after solar radiation at various places on the ground, i.e., the uneven heating of the earth's surface, the air pressure varies from place to place. Sunlight reaches the surface of the earth, so that the surface temperature rises, the air on the surface is heated to expand and rise. After the hot air rises, the cold air flows in laterally, and the rising air falls because it gradually cools and becomes heavier, and the air rises because the surface temperature is higher and heats up. This also creates wind. The total reserves of wind-energy resources are very large, with about  $5.3 \times 10^{13}$  kWh of exploitable energy, which is 10 times larger than the total amount of water energy available on earth [7]. Many countries have long begun to use wind-energy resources: the United States in 1974 on the implementation of the federal wind energy program; Denmark built the Jutland wind power station in 1978; Germany built a power station at the mouth of the Elbe River in 1980; and Japan built the largest indigenous wind-power station in Aomori Prefecture on the Karatsu Strait. Wind-power projects are also accelerating in countries across Asia, with Thailand utilizing twice as much wind energy in 2013 as in the previous year. The monsoon is the basic characteristic of China's climate, and China has ample reserves of wind-energy resources. Therefore, the utilization of wind-energy resources can be stepped up to make wind-energy resources the main power source in the world. Wind-energy resources, on the other hand, are largely concentrated in the diminishing areas of the Western Pacific and open continents due to topography, weather, time, and other factors [8]. Wind speed is the most important component determining wind energy because the amount of wind energy is related to the cube of wind speed. As a result, in order to maximize the acquisition of wind-energy resources, it is also required to screen wind speed from multiple perspectives. In summary, this paper analyzes and studies the characteristics of regional wind-energy-resource changes utilizing the Pettitt test and multi-variate empirical orthogonal function analysis (MV-EOF) and predicts the changing trend of wind speed by using the SARIMA model with the help of a multi-information data set from 2000 to 2021.

## 2. Materials and Methods

### 2.1. Materials

The geographical coordinates of East Asia and the Western Pacific region lie between  $0^{\circ}$  N to  $55^{\circ}$  N and  $70^{\circ}$  E to  $150^{\circ}$  E and include China, Korea, Mongolia, Japan, and North Korea. East Asia is located in the eastern part of Asia and on the west coast of the Pacific Ocean. East Asia is also in the Asian monsoon region and is a high greenhouse-gas emission area, which makes the variation in wind energy in the region have distinct regional characteristics. Wind-power generation is also affected by wind speed. Wind speed is converted into power by a wind turbine's characteristic curve. The same principle applies to forecasting wind speed and wind power [9]. This article analyzes the spatial and temporal variability in wind-energy resources in the study area using a multi-wind-energy resource dataset, with a special focus on the multi-year characteristics of the Western Pacific and open-continent contraction zones of East Asia.

The fifth-generation reanalyses of the European Centre for Medium-range Weather Forecasting (ERA5), National Centers for Environmental Prediction/National Center for Atmospheric Research (NCEP/NCAR), and the Integrated Global Radiosonde Archive (IGRA) of National Climatic Data Center (NCDC) are used in this study. This study encompasses the period 2000 to 2021. There are almost 1700 sounding sites in IGRA. This data is a collection of site data with a high spatial and temporal density and a good amount of detail. As shown in Figure 1a, the IGRA data covers most of East Asia in the study area, and the distribution of IGRA stations is shown in Figure 1a; topography map of the research area is shown in Figure 1b.

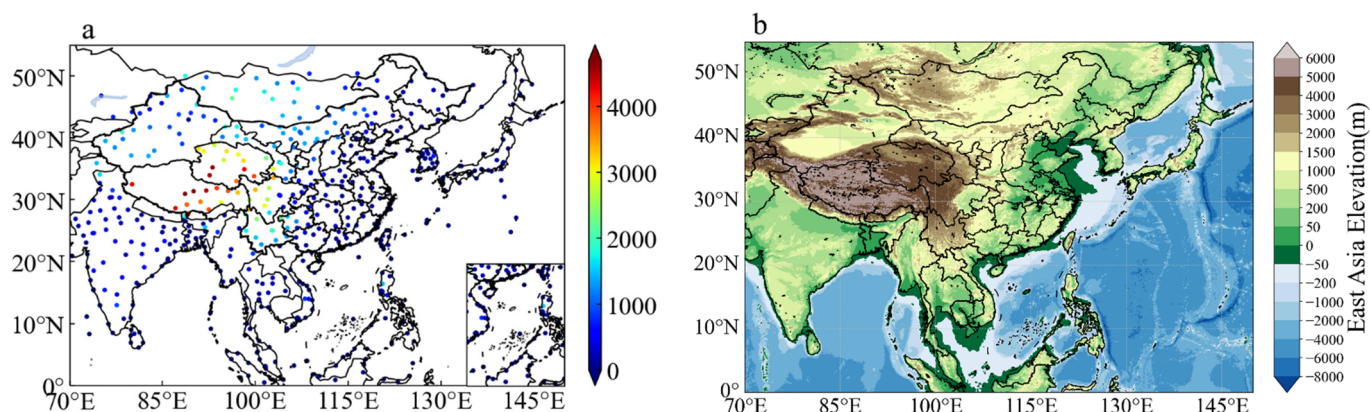


**Figure 1.** Study area: (a) distribution of IGRA sites within the East Asia region (IGRA data); (b) elevation map.

### 2.2. Methods

In this paper, inverse distance weighting interpolation, the Pettitt test, MV-EOF analysis, and other methods are applied. The main reason for choosing inverse distance-weighted interpolation in this paper is that it has a relatively simple formula and is especially suitable for site data with scattered nodes. After comparing the plot with other similar interpolation methods, it is easy to find that this paper prefers to use the inverse distance-weighted interpolation method. Inverse distance-weighting interpolation is a sort of weighted average interpolation. Data from each sounding site near the unmeasured point should be interpolated. By writing code in Python, the numerical site data is filled with the longitude and latitude points without numerical values. The inverse distance weight method mainly relies on the power value of the inverse distance, and controls the influence of known points on interpolation based on the distance from the output point. Grid data for wind-energy resources in the study area can be obtained by giving nearby stations large weights and distant stations small weights [10]. The main reason for choosing the Pettitt mutation point detection in the paper is that the Pettitt test has a better test for the mean change point at the endpoint location. In addition, the Brown–Forsythe test is more suitable for small

sample data. The Pettitt mutation test is a non-parametric mutation test that indicates the mutation year of the wind-energy resource [11]. The MV-EOF decomposition method is a simultaneous analysis of multiple parameters [12]. In this paper, two factors, wind speed and potential height, are analyzed under the same time coefficient series, and the correlation between the factors is analyzed step by step.

### 2.2.1. Pettitt Mutation Test

Pettitt mutation test is a nonparametric mutation test method. The algorithm's specific basis is as follows: for a known time series  $X(t), t = 1, 2, 3, \dots, n$ . Assume that there is a change point at  $t = \tau$ , which corresponds to the distribution function  $F_1(x)$  for the sequence  $X(t), t = 1, 2, 3, \dots, \tau$  before the mutation, and another distribution function  $F_2(x)$  for the sequence  $X(t), t = \tau, \tau + 1, \tau + 2, \dots, n$  after the mutation, and  $F_1(x)$  and  $F_2(x)$  are not equal. The statistic  $k(\tau)$  is checked by deducting sequence data before and after the mutation point using a rank-based comparison, and its formula is shown in Equation (1).

$$k(\tau) = \sum_{i=1}^{\tau} \cdot \sum_{j=\tau+1}^n \operatorname{sgn}(x_j - x_i), \quad (1)$$

In order to determine the absolute maximum time of  $k(\tau)$ , two statistics were defined as:

$$T = \tan^{-1} \max(|k(\tau)|), \quad K = \max(|k(\tau)|), \quad (2)$$

In the formula:  $K$  refers to the final Pettitt statistic;  $T$  refers to the corresponding unknown change point, with which the probability of significance can be approximated as:

$$P \approx 2 \exp \left[ -6K^2 (i^3 + i^2) \right]. \quad (3)$$

The change is generally considered significant when  $P < 0.5$ ; the sequence data are mutated at that point.

### 2.2.2. Multi-Variate Empirical Orthogonal Function

Multi-variate empirical orthogonal function (MV-EOF) can compress and analyze multiple variable fields to obtain spatial distribution patterns of variable fields with the same time coefficient, which is suitable to study the evolution of different variable fields over time and has advantages in simultaneously representing the spatial distribution of elements and the spatial connection between elements. The MV-EOF method can not only extract the main modes of wind-speed changes from multiple sets of reanalysis data, but it can also compare and analyze the similarities and differences in the spatial distribution patterns of the main modes in each set of data, and diagnose the data's quality and credibility.

Consider there are  $I$  variables, each with  $J$  spatial points and  $K$  time points, combined as  $Y = y_{ijk}$ . Where  $i = 1, \dots, I, j = 1, \dots, J, k = 1, \dots, K$ ,  $y_{ijk}$  means the normalized  $K$  observation of the  $I$  variable at the  $J$  spatial point distance level value.

### 2.2.3. Seasonal Autoregression Integrated Moving Average

Seasonal autoregression integrated moving average (SARIMA) model is used to predict the seasonal time series for the next few years by turning the wind speed into a stochastic series. When the stochastic series has a strong seasonal cyclic variation, it can be seasonally differentiated, and then the autocorrelation and partial correlation function plots of the first-order seasonal differential series of monthly mean wind speed from 2002 to 2020 and the differential score are used to determine the model parameter values and build the model for forecasting. This model can predict the future values based on the past and present values of the time series.



### 3. Results

#### 3.1. Temporal Variation Characteristics of Wind-Energy Resources in East Asia and Western Pacific Areas

Since East Asia is a high emitter of global greenhouse gases, we focus our analysis on wind-energy resources in this region. Figure 2 shows the inter annual variation in wind-energy resources in East Asia and the Western Pacific region from 2000 to 2021. Figure 2a specifically shows the four seasons and annual average trends for the last 22 years.

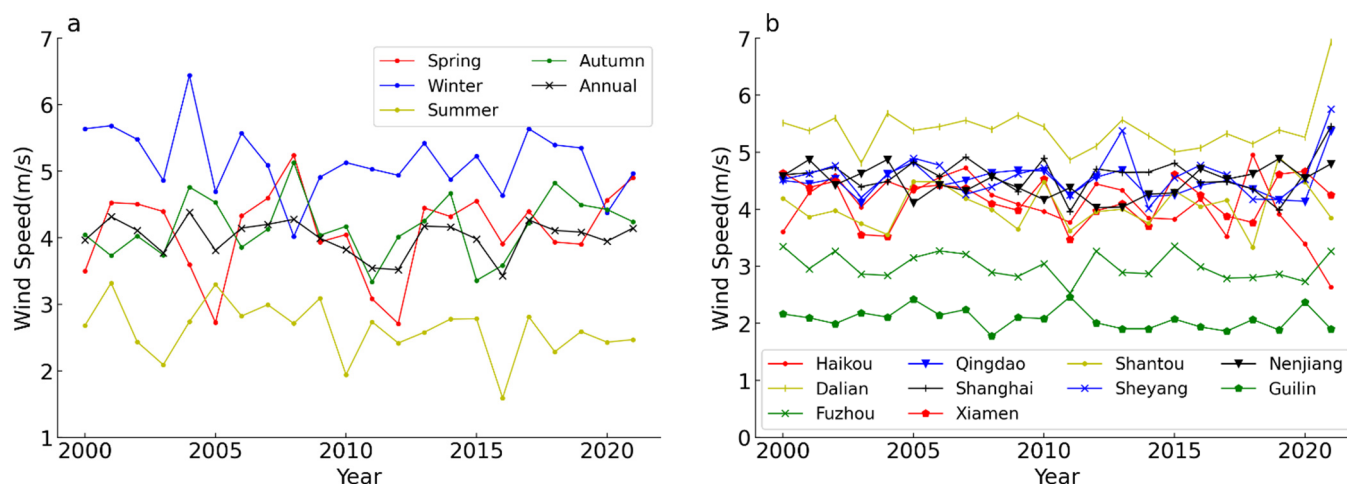


**Figure 2.** Temporal variation of wind speed resources in East Asia and Western Pacific areas (IGRA data): (a) multi-year average and four-season average trends; (b) site wind-speed map.

From Figure 2a, we can see that the average speed in summer is 2.62 m/s, the smallest among the four seasons; the minimum wind speed in summer is as low as 1.59 m/s, and the maximum wind speed in summer is 3.32 m/s, and the wind speed in summer has a tendency to decrease [13]; in winter it is 5.15 m/s, the largest among the recorded values; the minimum wind speed in winter is 4.02 m/s, and the maximum wind speed in winter is 6.44 m/s; the wind speeds in spring and autumn are 4.10 m/s and 4.16 m/s. The average values of wind speed in spring and autumn are 4.10 m/s and 4.16 m/s, respectively, and the variation in it in spring and autumn is similar, with an average value of 4.01 m/s throughout the year. Several Western Pacific sites and some inland sites are also selected for analysis in this paper, and Figure 2b specifically depicts the wind-speed variation maps of the sites from 2000 to 2021, and Figure 2b depicts ten areas with typical significance, namely, Haikou, Dalian, Fuzhou, Qingdao, Shanghai, Xiamen, Shantou, Qingdao, Shanghai, Xiamen, Shantou, Sheyang, Nengjiang, and Guilin. Table 1 shows the specific descriptions of the station numbers, data times, annual average wind speeds, and latitudes and longitudes for these 10 stations.

**Table 1.** Annual mean wind speed at stations in East Asia and Western Pacific areas.

(IGRA) Station	Year	Mean Wind Speed (m/s)	Latitude	Longitude
59,758 Haikou	2000~2021	4.08	20.000° N	110.250° E
54,662 Dalian	2000~2021	5.40	38.900° N	121.633° E
58,847 Fuzhou	2000~2021	3.00	26.083° N	119.283° E
54,857 Qingdao	2000~2021	4.50	36.066° N	120.333° E
58,362 Shanghai	2000~2021	4.60	31.416° N	121.450° E
59,134 Xiamen	2000~2021	4.17	24.483° N	118.083° E
59,316 Shantou	2000~2021	4.05	23.350° N	116.666° E
58,150 Sheyang	2000~2021	4.60	33.750° N	120.300° E
50,557 Nengjiang	2000~2021	4.48	49.166° N	125.233° E
57,957 Guilin	2000~2021	2.08	25.333° N	110.300° E

From Table 1, we can see that the annual mean wind speed of most Western Pacific areas from 2000 to 2021 is larger than that of other areas, and the mean wind speed of selected multiple sites is 4.01 m/s, which has a small error compared to the ERA5 data provided by the study area ECMWF [14]. Overall, it seems that the multi-year mean wind speed variation in Figure 2a is not significant, and, combined with Figure 2b, the multi-year mean wind speed variation in various places is limited, which indicates the stability of wind-energy resources in the study area and facilitates the in-depth investigation of their multifaceted energy storage. Locally, the wind resources are abundant in winter and insufficient in summer, mainly because the study area of this paper is a typical monsoon climate, and the summer wind is controlled by subtropical high pressure [15]. The subtropical high affects the summer monsoon, and the intensity of the subtropical high is linked to the thermal effect of solar radiation. The difference in atmospheric pressure due to the difference in the heating of land and sea by the sun leads to the formation of monsoons. Monsoons are generated by the combination of atmospheric circulation, land and sea distribution, and topographic surface. The winter winds and summer winds in the study area of this paper have different origins, and the weather phenomena show distinct seasonal differences due to the nature of the different air masses. Winter winds are mainly caused by the Mongolian high pressure; summer winds are mainly influenced by the southwest monsoon, southeast trade winds, and subtropical monsoon, respectively, but, due to the rotation effect of the Earth, the airflow is also influenced by the geotropic deflection force during the movement, which makes the winter winds concentrated and abundant, and the summer winds are slightly inferior in comparison, while the monsoon in East Asia is more complex mainly because it is influenced by the topographic effect of the Qinghai-Tibet Plateau and other factors [16].

To further investigate whether there are years of sudden changes in wind-energy resources in the region, we applied the Pettitt mutation test to perform mutation analysis for East Asia and Western Pacific areas. According to Figure 3a–d, it can be seen that the Pettitt mutation test for the average wind speed in each season of the last 22 years in East Asia and the Western Pacific region from 2000 to 2021 has mutations in 2013, 2009, 2018, and 2021; according to Figure 3e, it can be seen that the average annual wind Pettitt mutation test in 2021 exhibits a sudden change.

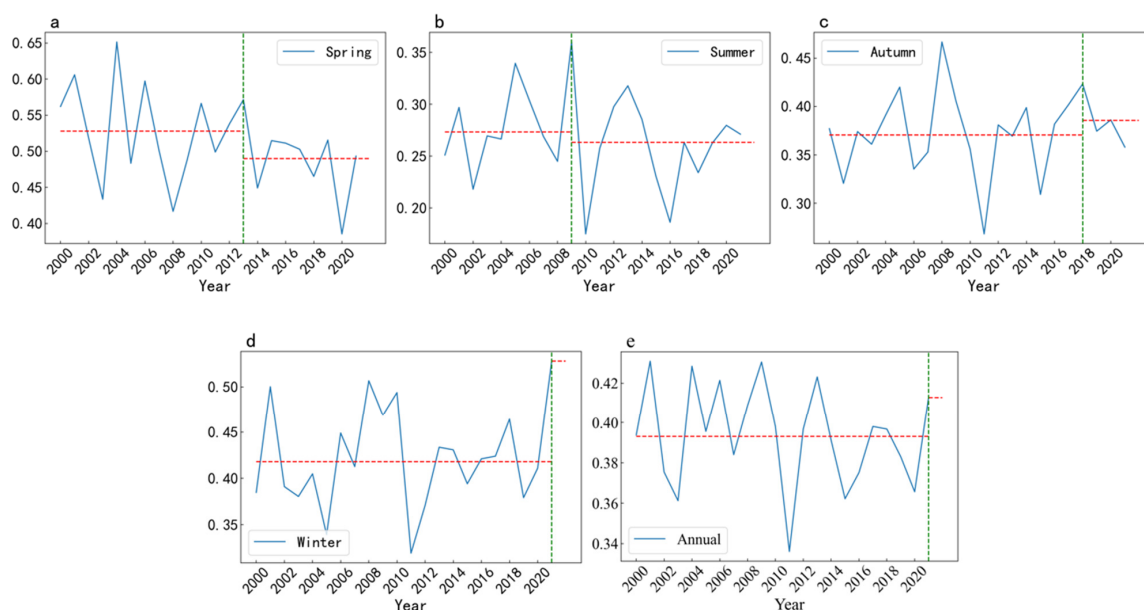


**Figure 3.** Pettitt mutation detection (IGRA data): (a) spring; (b) summer; (c) autumn; (d) winter; (e) annual mean. The spring mutation was near 2013, the summer mutation was near 2009, the fall mutation was near 2018, and there were no mutations in winter or throughout the year.

### 3.2. Spatial Variation Characteristics of Wind-Energy resources in East Asia and Western Pacific Areas

Combined with Figure 2a, which shows the seasonal variation in wind-energy resources in the study area, Figure 4 shows the seasonal spatial distribution of the average wind speed in East Asia and Western Pacific regions from 2000 to 2021. Among them, Figure 4a shows the spatial distribution of the average wind speed in spring. The western part of the Tibetan Plateau, Inner Mongolia, Xinjiang, and the southwestern part of Mongolia are the areas with large values of wind speed in the study area [17]; Figure 4b shows the distribution of the speed in summer, and the overall average wind speed is lower than the other three seasons, mainly because of the significant monsoon climate in the Western Pacific areas and the dual influence of the monsoon and atmospheric circulation. Figure 4c shows the spatial distribution of the average wind speed in autumn. The eastern part of Inner Mongolia, Qinghai-Tibet Plateau, and southern Xinjiang are areas with large values of wind speed, which is similar to the distribution of wind-energy resources in spring [18]. In the winter, Figure 4d depicts the regional distribution of average wind speed [19]. The Qinghai-Tibet Plateau in China, eastern Inner Mongolia, and southeastern Mongolia have the highest wind speeds. The wind speed is higher than in the prior three monsoons [20]. The main reason for this is that wind-energy supplies in the winter are primarily sourced from the chilly northern Eurasian continent, Siberia, and Mongolia. In addition, in the winter, heat escapes quickly on land, temperatures are low, pressure differences across geographical areas arise, and the wind is severe [21]. Combined with Figures 2a and 4a–d, the wind-energy resources in East Asia and Western Pacific areas are not only seasonally variable but also spatially and temporally disparate [22]. In addition, wind energy is more abundant in autumn and winter, less so in spring and summer, and significantly less in summer than in winter [23].

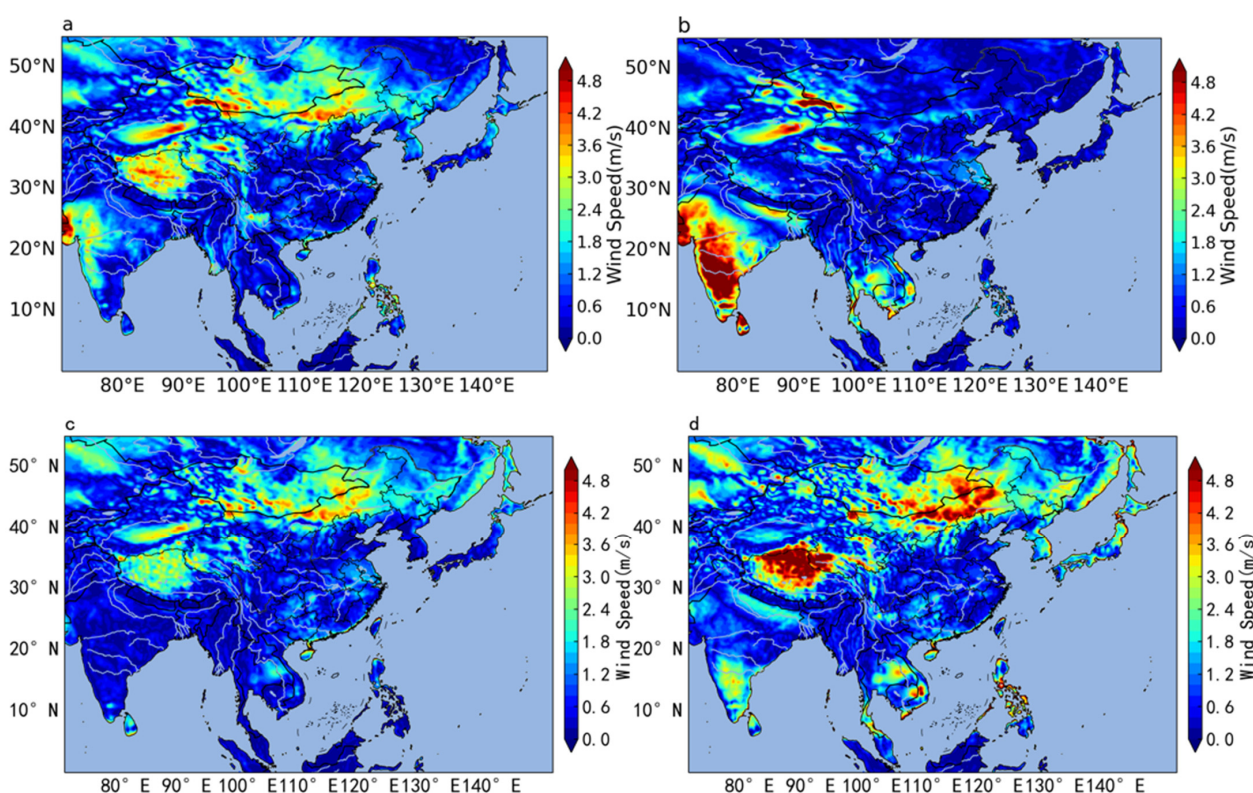


**Figure 4.** Seasonal spatial distribution of mean wind speed in East Asia and Western Pacific regions from 2000 to 2021 (reanalysis data): (a) spring; (b) summer; (c) autumn; and (d) winter.

In the comparison of ERA5 and NCEP data on geopotential height quality, NCEP data is highly consistent with the trend of sounding data [24]. Therefore, the superimposed



field of wind speed and geopotential height is studied, and we use NCEP data. Figure 5 shows the superimposed fields of wind energy and geopotential height in East Asia and the Western Pacific region from 2000 to 2021. Among them, Figure 5a shows the wind speed and geopotential height at 1000 hPa, and Figure 5b shows the speed at 925 hPa. On the whole, the wind speed for a large value area is mainly shown near 35°N [25], the wind direction is mainly northeasterly on the Qinghai-Tibet Plateau, and the direction is mainly northerly on the land of East Asia with Mongolia as the center of the pressure, while the direction is anti-southwesterly on the western Pacific Ocean [26], resulting in sufficient wind energy in the Qinghai-Tibet Plateau region, Xinjiang region, Inner Mongolia region, and Mongolia region of China. In the study area of this paper (0° N~55° N), the potential height gradually increases with the increase in latitude. Locally, the wind field at 1000 hPa is directly influenced by the Mongolia-centered air pressure, and the field at 925 hPa is doubly influenced by the East Asian monsoon circulation and the Mongolia-centered air pressure [27]. Except for the areas with sufficient wind power in Figure 5a, the wind power in the western Pacific and Western Pacific areas at the same latitude is also relatively sufficient [28].

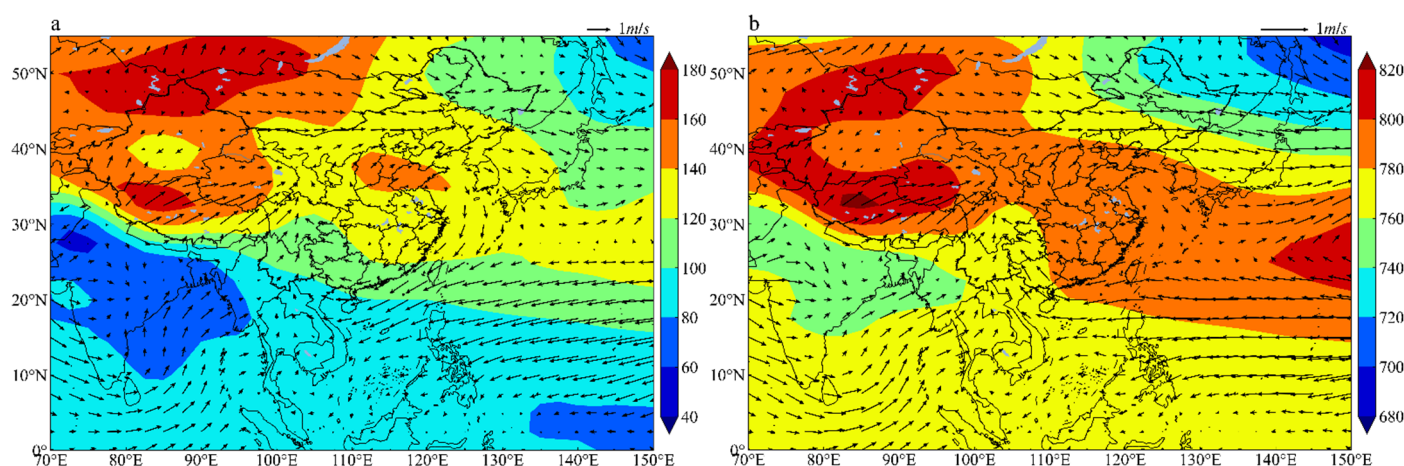


**Figure 5.** Wind vector and geopotential height superposition field in East Asia and Western Pacific region from 2000 to 2021 (reanalysis data): (a) 1000 hPa; and (b) 925 hPa.

### 3.3. MV-EOF Analysis of Annual Mean Wind Speed Variation

To further assess the wind-energy resources in the study area, the MV-EOF decomposition was performed by integrating the geopotential height and wind speed. The above analysis showed similarities in the patterns of geopotential height and wind-field distribution, but there were also significant seasonal differences in the circulation situation and magnitude [26]. Therefore, the analysis was performed for summer and winter. Figure 6 shows the spatial and temporal distribution of the first mode of wind speed and geopotential height for East Asia and Western Pacific regions from 2000 to 2021. Figure 7 shows the spatial and temporal distribution of the second mode of wind speed and geopotential height for East Asia and Western Pacific regions from 2000 to 2021. The cumulative variance contributions of the first two modes of wind speed and potential height are 37.78% and 50.44%, respectively. Among them, the sign of the coefficients in the temporal coefficients determines the direction of the mode, with a positive sign indicating the same direction as the mode and a negative sign the opposite, and a larger absolute value of the coefficients indicates the more typical form of the distribution for that year. Figure 6(a1–c1) and Figure 6(a2–c2) present the spatial distribution and time coefficients of wind speed and geopotential height in the first mode in summer and winter. The first-mode variance contribution of wind speed is 29.47% and the first-mode variance contribution of geopotential height is 37.75%, and the first mode characterizes the most important distribution characteristics of the speed and the height in the study area. The Qinghai-Tibet Plateau region of China has negative values in Figure 6(a1), whereas the western Pacific Ocean and



Western Pacific China have positive values. The main reason for this is that, during the summertime, the continent is exposed to the sun and the temperature warms up rapidly, forming low pressure near the ground while the ocean forms high pressure, and the East Asia region is controlled by summer winds; in Figure 6(a2), China's Qinghai-Tibet Plateau, Xinjiang region and part of Mongolia have positive values, while most of the Western Pacific region has negative values. The main reason for this is that, in winter, the wind mainly comes from the northern parts of the Asian and European continents in the severe cold of Siberia and Mongolia, and the wind is stronger in winter [29]. In Figure 6(b1), the majority of the study areas have negative values and a small portion have positive values, indicating that the spatial variation in potential height under this mode follows the same trend in most areas; in Figure 6(b2), the majority of Mongolia, some parts of Inner Mongolia, and South China have positive values, while the remainder has negative values. Figure 6(c1) and Figure 6(c2), respectively, show the time coefficients in summer and winter. Figure 6(c1) is negative from 2007 to 2015, and the remaining years are positive, indicating that wind speed as a whole is increasing in summer [30]. Figure 6(c2) is negative from 2001 to 2005, and the years have alternating positive and negative phases, mostly positive, and the time coefficients are increasing.

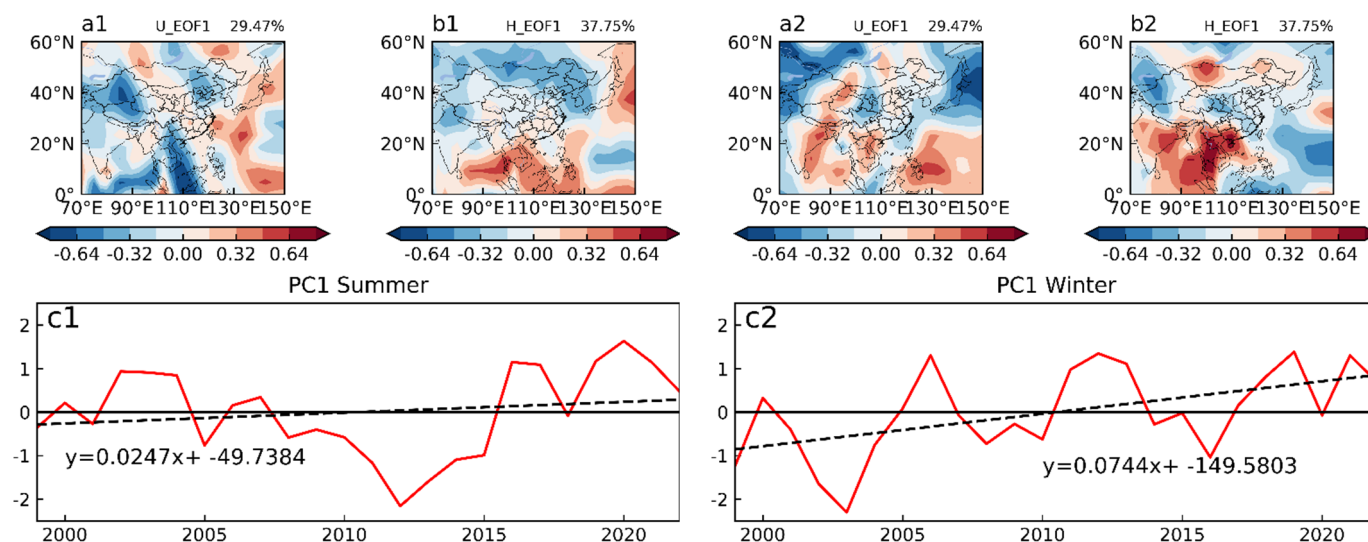


**Figure 6.** Spatial and temporal distribution of wind speed and geopotential height first mode in East Asia and Western Pacific region from 2000 to 2021 (reanalysis data): (a1) spatial distribution of summer wind speed; (b1) spatial distribution of summer geopotential height; (a2) spatial distribution of winter wind speed; (b2) spatial distribution of winter geopotential height; (c1) summertime coefficient; and (c2) wintertime coefficient.

Figure 7(a1–c1) and (a2–c2) depict the spatial and temporal distributions of wind speed and geopotential height in the second mode during the summer and winter seasons. The contribution of the second-mode variance in wind speed is 8.31% and the contribution of the second-mode variance in geopotential height is 12.69%. The study area in Figure 7(a1) has a positive distribution in summer and a negative distribution in winter, indicating that the second-mode spatial variance in wind speed is uniform, rising or falling at the same time; similarly, most areas in Figure 7(b1,b2) have positive distribution and a few are negative, indicating that the second-mode spatial variance of geopotential height is consistent. There is consistency. The time coefficients of summer and winter are shown in Figure 7(c1,c2), respectively, and Figure 7(c1,c2) alternate in positive and negative phases during the 22 years from 2000 to 2021. From the linear trend of the time coefficients of this mode, the trend of Figure 7(c1) is decreasing, which indicates a decreasing trend of summer wind speed in the study area over 22 years. The trend in Figure 7(c2) is increasing, which indicates an increasing trend of winter wind speed in the study area over 22 years, which is consistent with the decreasing trend of summer wind speed in Figure 2.

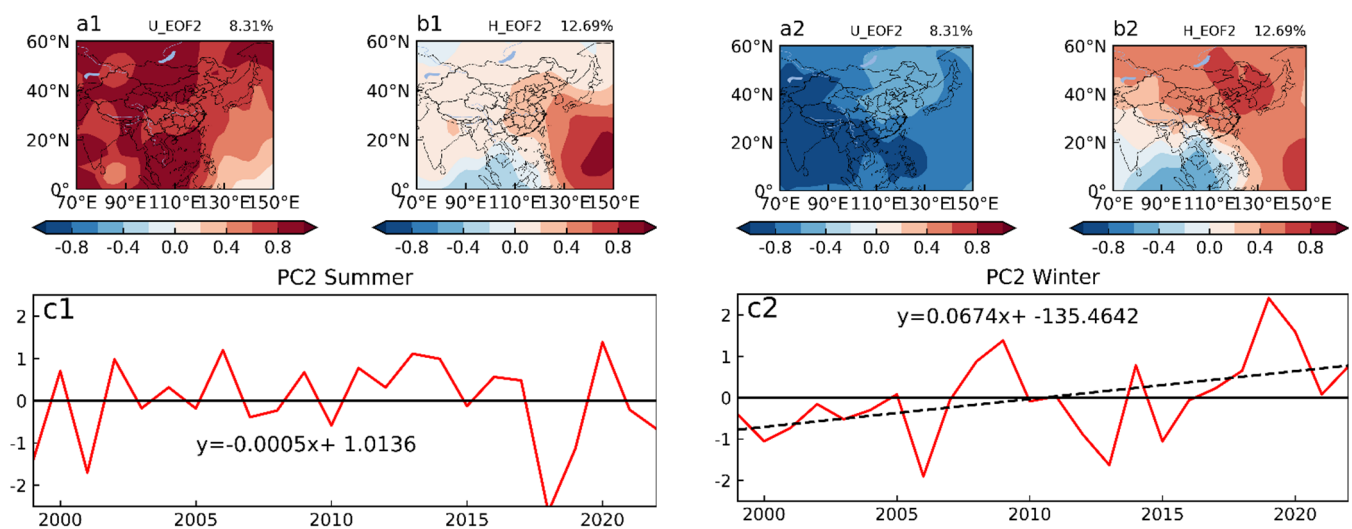


**Figure 7.** Spatial and temporal distribution of the second mode of wind speed and potential height in East Asia and Western Pacific region from 2000 to 2021 (reanalysis data): (a1) spatial distribution of summer wind speed; (b1) spatial distribution of summer potential height; (a2) spatial distribution of winter wind speed; (b2) spatial distribution of winter potential height; (c1) summertime coefficient; and (c2) wintertime coefficient.

### 3.4. Analysis of the Main Factors of Wind-Energy Resources in East Asia and Western Pacific Areas

The wind is a natural phenomenon caused by gas movement caused by the temperature difference caused by solar flow radiation, resulting in the rise and fall of hot and cold air in the vertical plane. According to prior studies, surface temperature, relative humidity, surface pressure, and total precipitation are more essential for wind-energy resources, according to prior studies, and are the key elements that influence wind-energy-resource variability [31]. As shown in Figure 8, the X-axis indicates the year, and the left side of the Y-axis indicates the wind speed.

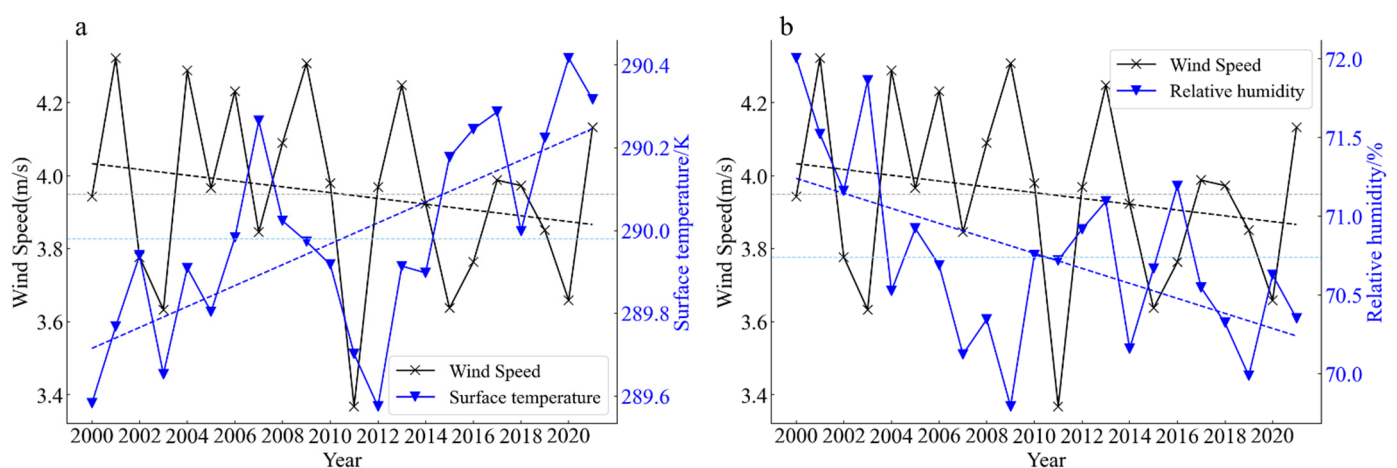


**Figure 8.** Trend variation in wind resource impact factors (reanalysis data): (a) wind speed and average temperature; and (b) wind speed and relative humidity.

Expanding the analysis further, the wind speed in Figure 8a shows a decreasing trend until 2010, but an increasing trend after 2010 [32], and, eventually, an overall increasing trend, which is consistent with the Pettitt test analysis of wind speed, above. In addition, through the significance test of the wind speed and the parameters mentioned above, combined with Table 2, it is found that only the wind speed fails to pass the significance

test of 0.01. In addition, the continued accelerating trend of the speed is a boon for the wind-power industry.

**Table 2.** Significance test of wind speed.

Parameter	Test for Significance
Wind speed	Not significant
Average temperature	Significant
Relative humidity	Significant
Surface pressure	Significant

As can be seen in Figure 8a, the wind speed shows a decreasing trend and the surface temperature shows an increasing trend, mainly due to the changes in large-scale oceanic and atmospheric circulation patterns caused by global warming [33]. As shown in Figure 8b, the wind speed shows a decreasing trend and the humidity also shows a decreasing trend. The main reason for this is that when the humidity is higher, the air here tends to be heavier and when the wind is stronger; the air will be blown to higher altitudes causing the humidity in the air to rise, so the higher the wind speed, the higher the relative humidity [34].

### 3.5. Forecast

Through the comparison of univariate wind-speed prediction models, this paper selects a single prediction model, SARIMA, to infer wind-speed variation trends and future predictions in East Asia, which can achieve good prediction results in wind-speed prediction and is often used as a reference model. In Figures 9 and 10, it is consistent with the findings already found in the previous section that the wind speed has started to increase since 2010, and the wind speed shows a clear upward trend after 2010. After checking multiple sources, this is mainly related to events such as changes in large-scale oceanic and atmospheric circulation patterns due to global warming, which is also a joint effect of land and sea surface temperatures.

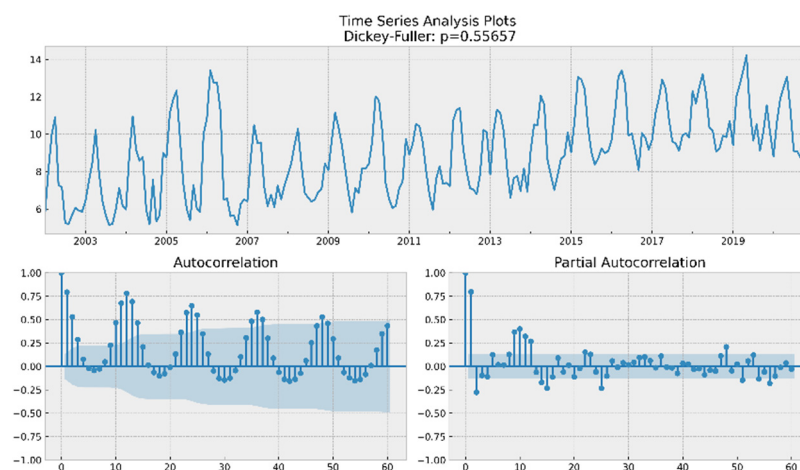


**Figure 9.** SARIMA raw graphs on wind speed data from 2002 to 2020 (reanalysis data. The blue line represents the wind speed).

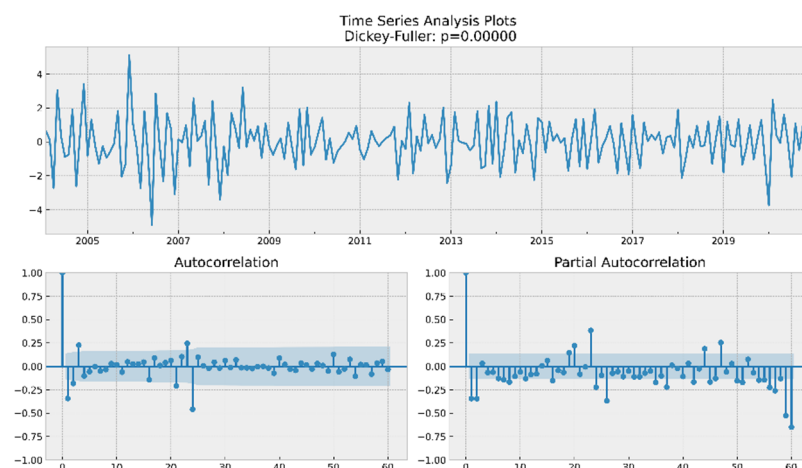


**Figure 10.** White noise test (reanalysis data. The blue line represents the wind speed).

Figure 11 shows the velocity values with the year on the  $x$ -axis and the annual average wind speed on the  $y$ -axis. Assume that the time series of wind speed is  $w(t), v(t) = w(t) - w(t-1), z(t) = v(t) - v(t-12), z(t) = a1 * z(t-1) + m(t) + b1 * m(t-1) + c1 * z(t-12) + d2 * m(t-24)$ , where  $w$  is the error term. The predictions are also applied to these equations, except that  $z(t)$  is predicted first, followed by  $v(t)$  and  $w(t)$ . The future values are predicted based on the past values, the present values, and the functional equations of the prediction. After 2020, the wind speed in East Asia and the Western Pacific continues the trend after 2012 and continues the upward trend, and there may be fluctuations in wind speed if major natural problems occur in or around that year. In addition, the average absolute percentage error is 8.81%, indicating that the SARIMA model is suitable for wind-speed prediction in this region.

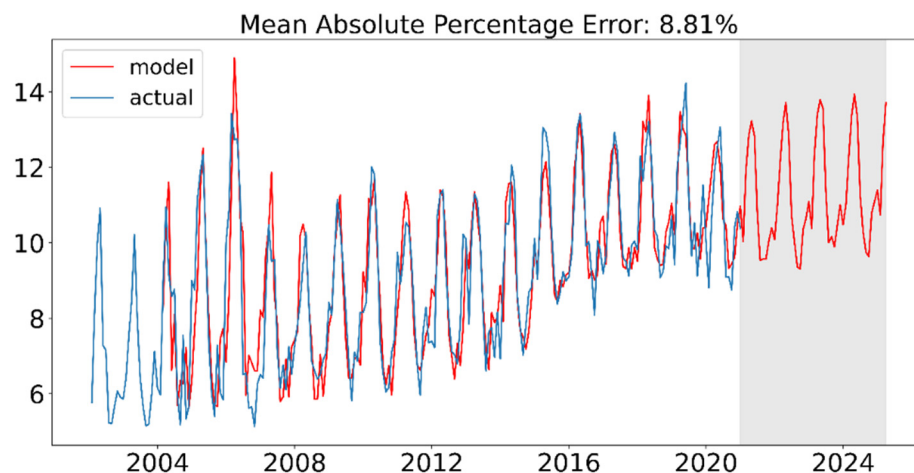


**Figure 11.** Plot of future 4-year data predicted using SARIMA for wind speed data from 2002 to 2020 (reanalysis data).

#### 4. Discussion

This paper finds that wind-energy resources in East Asia and Western Pacific regions are regionally distinctive. The abundant wind-energy resources are mainly concentrated in the three northern regions, the southeast coast, and Mongolia. It is also mentioned in several excellent papers referenced in this paper that, in the Chinese region, it is found that the spatiotemporal variability in wind resources in China is apparent and northeast China has the highest wind potential [17]. In addition, significant results show that the larger near-surface wind speed mainly occur in the northern and eastern regions, the Tibetan Plateau, and the Western Pacific zones in China [20]. This is consistent with the wind



resources studied in this paper and verifies the accuracy of the text. In addition, the winter monsoon and summer monsoon show obvious differences in seasonality mainly because of different air-mass properties, which is consistent with previous opinions. According to our paper, it is further found that the main reason why the East Asian monsoon is more complex is influenced by the topography of the Qinghai-Tibet Plateau and other factors. Finally, due to the significant geographical nature of the wind resources in the study area and the multiple combinations of comparisons with previous papers, this paper also demonstrates that the scaling of the study area is feasible and that more detailed areas of high wind resources can be delineated for more in-depth analysis in the future.

In the study area, there are also seasonal variances in the timing of wind-energy resources, according to this paper. The fundamental reason for this is that the ground obtains uneven amounts of solar radiation, resulting in substantial temperature fluctuations that cause monsoon activity to be uneven. This is also because wind speed in the near-surface layer is associated with climatic change circulation, which can be discovered essentially by observations, reanalysis, and ground-rotation wind theory analysis. According to the literature cited in this paper, annual surface wind speed (SWS) decreased from 1980 to 2012, with human activities being the most likely reason for the drop, while the improvement in the Asian meridional circulation was a key factor in the increase in SWS in winter [16]. Moreover, prior research has discovered a significantly decreased near-surface wind speed trend in China from 1979 to 2019, particularly between 1979 and 1996 [20]. The multi-year average wind speed showed a decreasing trend before 2010 and an increasing trend after 2010, when the study area and time range of this paper were combined [35]. Seasonal variability is significant, reflecting principally the impact of the East and Southeast Asia Monsoon, with higher speeds in winter, followed by summer, and weaker winds in autumn, followed by spring [22]. That opinion is supported by the finding of the study. Finally, recent studies imply that changes in near-surface wind speed are coupled to large-scale ocean-atmosphere circulations [25].

Ultimately, wind speed is strongly tied to diverse seasonal changes, with the changeable character of the weather and a higher degree of wind variability rendering wind prediction harder [6]. Although the reanalysis data used in this paper was still the highest resolution reanalysis data in the world, there are errors in the measurement process of the sounding data caused by natural or human factors, the topography of the study area is complex, and the vegetation cover near the ground is different, which also has an impact on the accuracy of the research results. For a more in-depth investigation, subsequent studies might be integrated with the topographic trend.

After grasping the wind resources, the impact of the wind-power industry on nature and human culture also needs to be considered. For example, the quality of life of local people and the adequacy of local unused land need to be considered, among other issues, which are the key considerations when wind resources are combined with wind-power plants [36]. Meanwhile, the research area of this paper is East Asia, and the research location can be gradually expanded in subsequent studies to obtain more experience of wind-power use.

## 5. Conclusions

Based on the sounding data from 2000 to 2021 and ERA5 and NCEP/NCAR reanalysis wind energy data, this paper carried out a spatial and temporal analysis of wind-energy resources in East Asia and Western Pacific areas using inverse distance weighted interpolation, Pettitt's mutation test, MV-EOF analysis methods, and used the SARIMA model to predict the trend of wind speed, and came to the following conclusions:

1. There are significant seasonal differences in wind-energy resources in the study area, with the lowest average wind speed of 1.59 m/s in summer and 6.44 m/s in winter. The wind speed is higher in autumn and winter and lower in spring and summer, and in summer it is significantly lower than in winter. The multi-year average wind speed decreased before 2010 and increased after 2010;

2. The mutation characteristics of the multi-year time series of the study area were analyzed using the Pettitt mutation test;
3. Combining the data from multiple sources, we found that wind energy in the East Asia and Western Pacific areas has significant regional characteristics, and wind-energy resources are richer in the Qinghai-Tibet Plateau, Inner Mongolia, Xinjiang, and Mongolia in China. The wind speed is strong in winter and spring in the Qinghai-Tibet Plateau, and weak in summer and autumn; Inner Mongolia has sufficient wind-energy resources in all seasons; and in the Xinjiang region, the wind speed is high in spring and summer compared with other regions, and minimal in winter;
4. Using the MV-EOF decomposition to analyze the study area, the first mode characterizes the most dominant distribution characteristics of the area. Within the study area, East Asia is controlled by summer winds in summer and by cold continental high pressure around Siberia and Mongolia in winter. In addition to this, the main reason for the more complex monsoon in East Asia is the influence of the topographic effect of the Tibetan Plateau and other factors.

**Author Contributions:** C.T.: Software, visualization and writing—review and editing. X.T.: Methodology, writing—original draft. Y.W.: funding acquisition and validation. Z.T.: investigation and resources. F.Z.: investigation and validation. H.L.: investigation and methodology. All authors have read and agreed to the published version of the manuscript.

**Funding:** This study is supported by the Graduate Innovation Foundation of Anhui University of Science and Technology (No. 2021CX2082; 2022CX2087; 2022CX2098), Anhui Province Key R&D Program of China under Grant (No. 202004i07020011), the scientific research start-up fund for high-level introduced talents of Anhui University of Science and Technology (No. 13190007), the University Natural Science Research Project of Anhui Province of China (No. KJ2019A0103), the Specialized Research Fund for State Key Laboratories (No. 201909), and the National key research and development program (No. 2017YFD0700501).

**Institutional Review Board Statement:** Not applicable.

**Informed Consent Statement:** Not applicable.

**Data Availability Statement:** The NCEP dataset of NCEP/NCAR was downloaded from <https://psl.noaa.gov/data/gridded/data.ncep.reanalysis> (accessed on 1 January 2022). The IGRA dataset of NCDC was downloaded from <ftp://ftp.ncdc.noaa.gov/pub/data/igra>. The ERA5 dataset of ECMWF was downloaded from <https://cds.climate.copernicus.eu>. (Recently accessed date: 25 March 2022).

**Acknowledgments:** We would like to thank the ECMWF, NCEP/NCAR, and NCDC team for providing the necessary datasets used in this study.

**Conflicts of Interest:** The authors declare that there are no conflicts of interest regarding the publication of this paper.

## References

1. Vaisi, S.; Alizadeh, H.; Lotfi, W.; Mohammadi, S. Developing the Ecological Footprint Assessment for a University Campus, the Component-Based Method. *Sustainability* **2021**, *13*, 9928. [\[CrossRef\]](#)
2. Xu, J.Z.; Assenova, A.; Erokhin, V. Renewable Energy and Sustainable Development in a Resource-Abundant Country: Challenges of Wind Power Generation in Kazakhstan. *Sustainability* **2018**, *10*, 3315.
3. Zhao, W.H.; Would, R.; Yuan, G.H.; Wang, H.; Tan, Z.F. Long-Term Cointegration Relationship between China's Wind Power Development and Carbon Emissions. *Sustainability* **2019**, *11*, 4625. [\[CrossRef\]](#)
4. Xu, B.; Lin, B.Q. A quantile regression analysis of China's provincial CO<sub>2</sub> emissions: Where does the difference lie? *Energy Policy* **2016**, *98*, 328–342. [\[CrossRef\]](#)
5. Zhang, L.; Liu, X.Y.; Ouyang, X.T.; Chen, W. Characteristic analysis of conventional pole and consequent pole IPMSM for electric vehicle application. *Energy Rep.* **2022**, *8*, 259–269. [\[CrossRef\]](#)
6. Salah, S.; Alsamamra, H.R.; Shoqair, J.H. Exploring Wind Speed for Energy Considerations in Eastern Jerusalem-Palestine Using Machine-Learning Algorithms. *Energies* **2022**, *15*, 2602. [\[CrossRef\]](#)
7. Wu, F.L.; Fang, C.L. Wind Power Resource Appraisal and Development Stage Regional Division of China. *J. Nat. Res.* **2009**, *24*, 1412–1421.

8. Ren, L.; Ji, J.C.; Lu, Z.J.; Wang, K. Spatiotemporal characteristics and abrupt changes of wind speeds in the Guangdong–Hong Kong–Macau Greater Bay Area. *Energy Rep.* **2022**, *8*, 3465–3482. [\[CrossRef\]](#)
9. Zivkovic, M.; Lazic, L.; Pejanovic, G. Wind forecasts for wind power generation using the Eta model. *Renew. Energy* **2010**, *35*, 1236–1243.
10. Guo, Q.Y.; Huang, R.; Zhuang, L.W.; Zhang, K.Y.; Huang, J.F. Assessment of China’s Offshore Wind Resources Based on the Integration of Multiple Satellite Data and Meteorological Data. *Remote Sens.* **2019**, *11*, 2680. [\[CrossRef\]](#)
11. Liu, X.M.; Zhang, D. Trend analysis of reference evapotranspiration in Northwest China: The roles of changing wind speed. *Hydrol. Process.* **2013**, *27*, 3941–3948. [\[CrossRef\]](#)
12. Shi, X.H.; Chen, J.Q.; Wen, M. The relationship between heavy precipitation in the eastern region of China and atmospheric heating anomalies over the Tibetan Plateau and its surrounding areas. *Theor. Appl. Climatol.* **2019**, *137*, 2335–2349. [\[CrossRef\]](#)
13. Liu, C.; Li, Q.L.; Zhao, W.; Wang, Y.Q.; Ali, R.; Huang, D.; Lu, X.X.; Zheng, H.; Wei, X.L. Spatiotemporal Characteristics of Near-Surface Wind in Shenzhen. *Sustainability* **2020**, *12*, 739. [\[CrossRef\]](#)
14. Feng, Y.C.; Que, L.J.; Feng, J.M. Spatiotemporal characteristics of wind energy resources from 1960 to 2016 over China. *Theor. Appl. Climatol.* **2020**, *13*, 136–145. [\[CrossRef\]](#)
15. Tseng, Y.H.; Lu, C.Y.; Zheng, Q.A.; Ho, C.R. Characteristic Analysis of Sea Surface Currents around Taiwan Island from CODAR Observations. *Remote Sens.* **2021**, *13*, 3025. [\[CrossRef\]](#)
16. Zheng, J.L.; Li, B.F.; Chen, Y.N.; Chen, Z.S.; Lian, L.S. Spatiotemporal variation of upper-air and surface wind speed and its influencing factors in northwestern China during 1980–2012. *Theor. Appl. Climatol.* **2018**, *133*, 1303–1314. [\[CrossRef\]](#)
17. Qiao, Z.; Wu, F.; Xu, X.L.; Yang, J.; Liu, L. Mechanism of Spatiotemporal Air Quality Response to Meteorological Parameters: A National-Scale Analysis in China. *Sustainability* **2019**, *11*, 3957. [\[CrossRef\]](#)
18. Chen, Z.; Li, W.; Guo, J.H.; Bao, Z.; Pan, Z.R.; Hou, B.D. Projection of Wind Energy Potential over Northern China Using a Regional Climate Model. *Sustainability* **2020**, *12*, 3979. [\[CrossRef\]](#)
19. Guo, J.H.; Huang, G.H.; Wang, X.Q.; Xu, Y.; Li, Y.P. Projected changes in wind speed and its energy potential in China using a high-resolution regional climate model. *Wind Energy* **2020**, *23*, 471–485. [\[CrossRef\]](#)
20. Li, X.; Pan, Y.J.; Jiang, Y.S. The analysis of the spatiotemporal variations and mechanisms for the near-surface wind speed over China in the last 40 years. *Theor. Appl. Climatol.* **2022**, *148*, 1163–1180. [\[CrossRef\]](#)
21. Diao, W.J.; Zhao, Y.; Dong, Y.Y.; Zhai, J.Q.; Wang, Q.M.; Gui, Y.P. Spatiotemporal Variability of Surface Wind Speed during 1961–2017 in the Jing-Jin-Ji Region, China. *J. Meteorol. Res.* **2020**, *34*, 621–632. [\[CrossRef\]](#)
22. Yu, L.J.; Zhong, S.Y.; Bian, X.D.; Heilman, W.E. Climatology and trend of wind power resources in China and its surrounding regions: A revisit using Climate Forecast System Reanalysis data. *Int. J. Climatol.* **2016**, *36*, 2173–2188. [\[CrossRef\]](#)
23. Guo, H.; Xu, M.; Hu, Q. Changes in near-surface wind speed in China: 1969–2005. *Int. J. Climatol.* **2011**, *31*, 349–358. [\[CrossRef\]](#)
24. Lin, C.G.; Yang, K.; Qin, J.; Fu, R. Observed Coherent Trends of Surface and Upper-Air Wind Speed over China since 1960. *Int. J. Climatol.* **2014**, *34*, 1873–1882. [\[CrossRef\]](#)
25. Li, X.; Li, Q.P.; Ding, Y.H.; Wang, M. Near-surface wind speed changes in eastern China during 1970–2019 winter and its possible causes. *Adv. Clim. Chang. Res.* **2022**, *13*, 228–239. [\[CrossRef\]](#)
26. Gao, M.; Yang, Y.; Shi, H.H.; Gao, Z.Q. SOM-based synoptic analysis of atmospheric circulation patterns and temperature anomalies in China. *Atmos. Res.* **2019**, *220*, 46–56. [\[CrossRef\]](#)
27. Lockwood, J.F.; Thornton, H.E.; Ren, H.L. Skilful seasonal prediction of winter wind speeds in China. *Clim. Dyn.* **2019**, *53*, 3937–3955. [\[CrossRef\]](#)
28. Zhang, R.H.; Zhang, S.Y.; Luo, J.L.; Han, Y.Y.; Zhang, J.X. Analysis of near-surface wind speed change in China during 1958–2015. *Theor. Appl. Climatol.* **2019**, *137*, 2785–2801. [\[CrossRef\]](#)
29. Lin, D.Y.; Huang, W.Y.; Yang, Z.F.; He, X.S.; Qiu, T.P.; Wang, B.; Wright, J.S. Impacts of Wintertime Extratropical Cyclones on Temperature and Precipitation Over Northeastern China During 1979–2016. *J. Geophys. Res.-Atmos.* **2019**, *124*, 1514–1536. [\[CrossRef\]](#)
30. Zhao, C.; Jiang, Z.H.; Sun, X.J.; Li, W.; Li, L. How well do climate models simulate regional atmospheric circulation over East Asia? *Int. J. Climatol.* **2020**, *40*, 220–234. [\[CrossRef\]](#)
31. Zhou, L.T.; Huang, R. Regional differences in surface sensible and latent heat fluxes in China. *Theor. Appl. Climatol.* **2014**, *116*, 625–637. [\[CrossRef\]](#)
32. Cui, X.J.; Dong, Z.B.; Sun, H.; Li, C.; Xiao, F.J.; Liu, Z.Y.; Song, S.P.; Li, X.L.; Xiao, N.; Xiao, W.Q. Spatial and temporal variation of the near-surface wind environment in the dune fields of northern China. *Int. J. Climatol.* **2018**, *38*, 2333–2351. [\[CrossRef\]](#)
33. Yu, J.; Zhou, T.J.; Jiang, Z.H. Interannual variability of the summer wind energy over China: A comparison of multiple datasets. *Wind Energy* **2020**, *23*, 1726–1738. [\[CrossRef\]](#)
34. Zeng, J.; Zhang, Q. A humidity index for the summer monsoon transition zone in East Asia. *Clim. Dyn.* **2019**, *53*, 5511–5527. [\[CrossRef\]](#)
35. Ge, J.; Feng, D.P.; You, Q.L.; Zhang, W.J.; Zhang, Y.Q. Characteristics and causes of surface wind speed variations in Northwest China from 1979 to 2019. *Atmos. Res.* **2021**, *254*, 105527. [\[CrossRef\]](#)
36. Johansson, M.; Laike, T. Intention to respond to local wind turbines: The role of attitudes and visual perception. *Wind Energy* **2007**, *10*, 435–451. [\[CrossRef\]](#)